


Effects of satellite lines in fittings of He-like triplets of X-ray Spectra

Lan Zhang¹ , Xiangxiang Xue^{1,2}, Dawei Yuan¹, Huigang Wei¹,
Feilu Wang¹⁻⁴ and Gang Zhao^{1,2}

¹Key Laboratory of Optical Astronomy, National Astronomical Observatories,
Chinese Academy of Sciences, Beijing 100012, China

²School of Astronomy and Space Science University of Chinese Academy of Sciences, Beijing
101408, China

³Graduate School of China Academy of Engineering Physics, Beijing, 100196, China

⁴email: wfl@nao.cas.cn

Abstract. We estimate the wind speeds with a Bayesian inference and a Markov Chain Monte Carlo (MCMC) tool for the high resolution X-ray spectra of Vela X-1, to understand the effect of satellite lines on spectral analysis. After modelling continua and He-like triplets of the spectra with a parameterized two-component power-law model and a multi-Gaussian model, respectively, we estimate the contamination from satellite lines, and improve the self-consistency of wind speeds derived from the He-like triplet lines of different elements. Moreover, our fitting shows that the column density of scatter component varies from phase to phase.

Keywords. methods: data analysis; X-rays: binaries; line: identification

1. Introduction

To understand the X-ray binary (e.g. Vela X-1), much information is derived from the X-ray spectral observations, such as the wind speed, the element abundance and temperatures. The derivation depends on fitting the observed spectra with χ^2 and Bayesian inference. The advantages of Bayesian analysis over χ^2 (Sako *et al.* 1999; Goldstein *et al.* 2004) are the inclusion of prior information of data, providing possible values and confidence intervals for each parameter (e.g., Reichart *et al.* 1999; Benítez 2000; Buchner *et al.* 2014; Walker *et al.* 2015).

Using the Bayesian analysis, it is possible to study the effect of satellite lines to He-like triplets on the derived physical information. He-like triplets are commonly used to diagnose the temperature and density (Porquet & Dubau 2000). And close to the triplets, there are some robust satellite lines. Due to the limited resolution, they overlap with their parent lines, which shift the triplets center and distort the line profile significantly (Wang *et al.* 2017).

In the present work, we take a well-studied X-ray binary, Vela X-1, as an example, to study this effect on the derived wind speeds. The satellite lines have been taken into account when we fit the observed He-like triplets with Bayesian analysis. The wind speeds, from the difference between the line at rest and fitted wavelength, show a good self-consistency among various lines. In addition, the error ranges are given from the fitted line profiles, which would be passed to the diagnosed temperature from the line ratio.

2. Method

For each parameter of a model fitted to a high resolution X-ray spectrum, we aim to marginalize the posterior probability density function (hereafter PDF) to derive the best fitted value and its corresponded uncertainty. In the Bayesian approach, the posterior PDFs of the model parameters for a given observed spectra, $F_{\text{obs}}(E)$, is

$$P(\mathbf{p}, b | F_{\text{obs}}(E)) = \frac{\mathcal{L}(F_{\text{obs}}(E) | \mathbf{p}, b) \times p(\mathbf{p}, b)}{\mathcal{L}(F_{\text{obs}}(E))} \quad (2.1)$$

(MacKay 2003). Where \mathbf{p} is a vector of parameters of a spectral model, b represents the background noise of a X-ray spectrum and $\mathcal{L}(F_{\text{obs}}(E))$ is the normalization independent of all the parameters.

$\mathcal{L}(F_{\text{obs}}(E) | \mathbf{p}, b)$ is the likelihood function of $F_{\text{obs}}(E)$ given the parameters $[\mathbf{p}, b]$, whose logarithm form can be written as

$$\ln \mathcal{L}(F_{\text{obs}}(E) | \mathbf{p}, b) = - \sum_{m=1}^M \ln(2\pi\delta_m^2) - \sum_{m=1}^M \frac{1}{2} \left[\frac{F_{\text{mod}}(E_m | \mathbf{p}) - F_{\text{obs}}(E_m)}{\delta_m} \right]^2 \quad (2.2)$$

where,

$$\delta_m = \sqrt{\epsilon_{\text{obs}}(E_m)^2 + b^2}, \quad (2.3)$$

M is the total data number used in spectral fitting, and $\epsilon_{\text{obs}}(E_m)$ is the error of the observed spectrum. In this analysis, the dataset of $F_{\text{obs}}(E)$ were observed with the *Chandra* HETG/ACIS-S – the High-Energy Transmission Grating/Advanced Imaging Spectrometer, during three different orbital phases centered on Eclipse, $\phi = 0.25$, and $\phi = 0.5$ in 2001, with *Chandra* ObsIDs 1926, 1928, and 1927, respectively. The observation and instrument details can be found in Paul *et al.* (2002); Sako *et al.* (2003) and Goldstein *et al.* (2004). $F_{\text{mod}}(E_m | \mathbf{p})$ is a parameterized spectral model, which is composed by a two component continuum emission model (Sako *et al.* 1999), having the form

$$F_{\text{cont}}(E) = A^{\text{scat}} \exp[-\sigma(E)N_{\text{H}}^{\text{scat}}] E_{\text{keV}}^{-\Gamma^{\text{scat}}} + A^{\text{dir}} \exp[-\sigma(E)N_{\text{H}}^{\text{dir}}] E_{\text{keV}}^{-\Gamma^{\text{dir}}}, \quad (2.4)$$

and a multi-Gaussian line model ($F_{\text{line}}(E)$), having the form

$$F_{\text{line}}(E) = \sum_{i=1}^n A_j \exp\left[-\frac{(E - E_j)^2}{2\epsilon_j^2}\right]. \quad (2.5)$$

Where n is the total number of lines fitted in each set of He-like line emission. Both F_{cont} and $F_{\text{line}}(E)$ are the energy-resolved photon flux.

$p(\mathbf{p}, b)$ is the prior function. Here we use a step function over each parameter

$$p(\mathbf{p}) = \begin{cases} \frac{1}{\mathbf{p}_{\text{upper}} - \mathbf{p}_{\text{lower}}}, & \text{if } \mathbf{p} \in [\mathbf{p}_{\text{lower}}, \mathbf{p}_{\text{upper}}] \\ 0, & \text{otherwise} \end{cases}, \quad (2.6)$$

$$p(b) = \begin{cases} \frac{1}{b_{\text{upper}}}, & \text{if } b \in (0., b_{\text{upper}}) \\ 0, & \text{otherwise} \end{cases}.$$

Selecting the $[\mathbf{p}_{\text{lower}}, \mathbf{p}_{\text{upper}}]$ and b_{upper} is different from case to case.

In this work, we adopt a stable, well-tested MCMC algorithm, *emcee* proposed by Foreman-Mackey *et al.* (2013) to the spectral study of Vela X-1. The algorithm of *emcee* is based on the Metropolis-Hasting method (Section 15.8 of Press 2007) and an affine-invariant ensemble sampling algorithm called the ‘‘stretch move’’ (Goodman & Weare 2010).

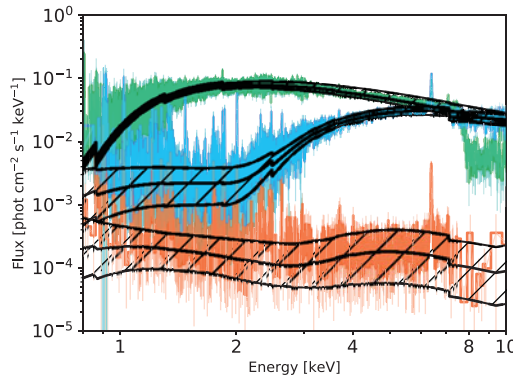


Figure 1. The best fitted continua and corresponding error ranges are shown in thick black lines and hatched areas. Observed spectra for Eclipse, $\phi = 0.25$, and $\phi = 0.5$ are represented by red, green, and blue steps, respectively.

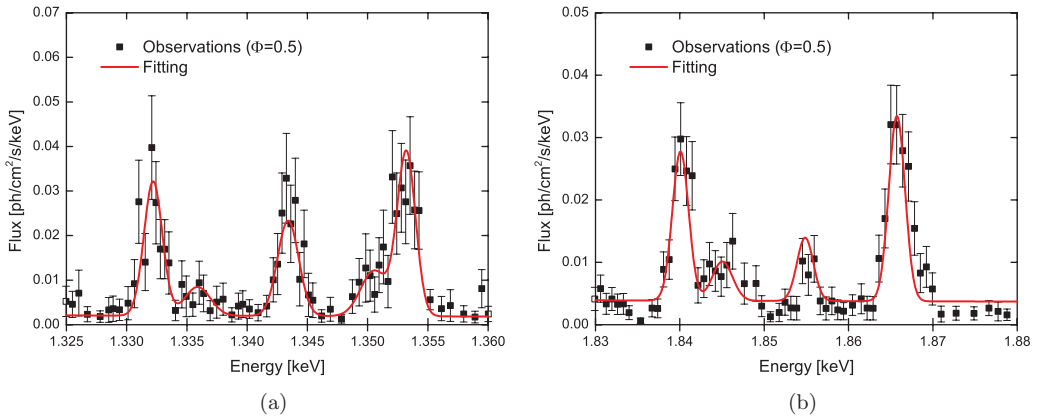


Figure 2. The best fitted He-like triplets, using spectra of $\phi = 0.5$ as examples.

3. Results

The best fitted F_{cont} are shown in Figure 1. For the column density of scatter component in the model (Sako *et al.* 1999), $N_{\text{H}}^{\text{scat}}$ are derived as $0.24^{+0.26}_{-0.16}$, $7.75^{+0.88}_{-0.92}$, and $0.22^{+0.13}_{-0.10}$ in 10^{22}cm^{-2} for $\phi = 0$, 0.25, and 0.5, respectively. This variation from phase to phase might imply a non-spherical structure of the stellar wind, which is in agreement with the simulation of Blondin *et al.* (1991).

Figure 2 gives the best fitting of the observed He-like triplets of silicon and magnesium. From the difference between the fitted wavelength and that at rest, we derived the wind speeds in km/s as 153^{+32}_{-33} and 132^{+27}_{-25} from resonance (r) and forbidden (f) lines, as well as 230^{+74}_{-91} and 153^{+96}_{-86} from intercombination (i) lines of Si. Compared with the previous results, this shows that considering the distribution of the satellites around would be helpful to improve the self-consistency within $1 - \sigma$ error region (Zhang *et al.* 2019).

In addition, due to the inclusion of satellite lines, the line flux derived is systematically lower. Also the continua and background effect would affect the line intensity determination, which are used to derive the abundance and the temperature with line ratios (i.e. $G(T_e) = (f + i)/r$).

4. Summary

In this work, we applied a Bayesian approach to the archive spectra of Vela X-1 with three different phases, $\phi = 0$, $\phi = 0.25$, and $\phi = 0.5$. We adopt a parameterized two-component power-law model and a multi-Gaussian model to predict the continua and He-like triplets, respectively, for all three phases, by setting all parameters as free. Then we fit the observed continua and He-like triplets of Mg 11 and Si 13, by using an MCMC algorithm, *emcee* to recover the posterior PDFs of all parameters of F_{cont} , F_{line} , and the background. In our results, the column density of scatter component $N_{\text{H}}^{\text{scat}}$ varies from phase to phase, which implies a non-spherical structure of stellar wind. Moreover, our measured wind velocities show very good self-consistency, which provide a reliable approach for the diagnostics of photoionized plasma in the future.

Acknowledgment

This work is supported by the National Natural Science Foundation of China (NSFC) (Nos. 11573040, 11773033, 11873052, and 11233004). X.X.X. acknowledges the support from the Recruitment Program of Global Youth Experts of China.

References

- Benítez, N. 2000, *ApJ* 536, 571
- Blondin, J. M., Kallman, T. R., Fryxell, B. A., & Taam, R. E. 1990, *ApJ* 356, 591
- Blondin, J. M., Stevens, I. R., & Kallman, T. R. 1991, *ApJ* 371, 684
- Buchner, J., Georgakakis, A., Nandra, K., Hsu, L., Rangel, C., Brightman, M., Merloni, A., Salvato, M., Donley, J., & Kocevski, D. 2014, *A&A* 564, A125
- Chung, H.-K., Chen, M., Morgan, W., Ralchenko, Y., & Lee, R. 2005, *HEDP* 1
- Ferland, G. J., Korista, K. T., Verner, D. A., Ferguson, J. W., Kingdon, J. B., & Verner, E. M. 1998, *PASP* 110, 761
- Foreman-Mackey, D., Hogg, D. W., Lang, D., & Goodman, J. 2013, *PASP* 125, 306
- Fujioka, S., Takabe, H., Yamamoto, N., Salzmann, D., Wang, F., Nishimura, H., Li, Y., Dong, Q., Wang, S., Zhang, Y., Rhee, Y.-J., Lee, Y.-W., Han, J.-M., Tanabe, M., Fujiwara, T., Nakabayashi, Y., Zhao, G., Zhang, J., & Mima, K. 2009, *Nature Phys.*, 5, 821
- Goldstein, G., Huenemoerder, D. P., & Blank, D. 2004, *AJ* 127, 2310
- Goodman, J., & Weare, J. 2010, *Communications in Applied Mathematics and Computational Science* 5, 65
- Han, B., Wang, F., Salzmann, D., & Zhao, G. 2015, *PASJ* 67, 29
- MacKay, D. J. 2003, in *Information theory, inference and learning algorithms* (Cambridge university press)
- Paul, B., Dewangan, G. C., Sako, M., Kahn, S. M., Paerels, F., Liedahl, D., Wojdowski, P., & Nagase, F. 2002, in: S. Ikeuchi, J. Hearnshaw, & T. Hanawa (eds.), *8th Asian-Pacific Regional Meeting*, Volume II, p. 355
- Porquet, D., & Dubau, J. 2000, *A&A* 143, 495
- Porquet, D., Dubau, J., & Grosso, N. 2010, *Space Sci. Rev.* 157, 103
- Press, W. H. 2007, *Numerical recipes 3rd edition: The art of scientific computing* (Cambridge university press)
- Reichart, D. E., Castander, F. J., & Nichol, R. C. 1999, *ApJ* 516, 1
- Sako, M., Kahn, S. M., Paerels, F., Liedahl, D. A., Watanabe, S., Nagase, F., & Takahashi, T. 2003, *ArXiv Astrophysics e-prints*, astro-ph/0309503
- Sako, M., Liedahl, D. A., Kahn, S. M., & Paerels, F. 1999, *ApJ* 525, 921
- Smith, R. K., Brickhouse, N. S., Liedahl, D. A., & Raymond, J. C. 2001, *ApJ* 556, L91
- Walker, M. G., Olszewski, E. W., & Mateo, M. 2015, *MNRAS* 448, 2717
- Wang, F., Han, B., Salzmann, D., & Zhao, G. 2017, *Physics of Plasmas* 24, 041403
- Watanabe, S., Sako, M., Ishida, M., Ishisaki, Y., Kahn, S. M., Kohmura, T., Nagase, F., Paerels, F., & Takahashi, T. 2006, *ApJ* 651, 421
- Zhang, L., Wang, F., Xue, X., Yuan, D., Wei, H. & Zhao, G. 2019, *High Power Laser Science and Engineering* 6, e37